J. Min. Metall. Sect. B-Metall. 54 (1) B (2018) 51 - 57

Journal of Mining and Metallurgy, Section B: Metallurgy

EFFECT OF ELECTROSLAG REMELTING ON THE NON-METALLIC INCLUSIONS IN H11 TOOL STEEL

J. Burja [a, *], F. Tehovnik [a], M. Godec [a], J. Medved [b], B. Podgornik [a], R. Barbič [c]

[a] Institute of Metals and Technology, Ljubljana, Slovenia,
[b] University of Ljubljana, Faculty of Natural Sciences and Engineering, Ljubljana, Slovenia
[c] Rok Barbič, Metal d.o.o., Ravne na Koroškem, Slovenia

(Received 23 June 2016; accepted 22 December 2017)

Abstract

We have studied the effect of electroslag remelting on the content and composition of non-metallic inclusions. It was found that a decrease in the non-metallic inclusion content occurred during the electroslag remelting. A change in the chemical composition of the non-metallic inclusions was observed, while the aluminum and calcium contents were increased. The complexity of the inclusions also increased, as there were fewer single-phase inclusions after the electroslag remelting process. Based on the results and a thermodynamic assessment of the formation of the non-metallic inclusions, a mechanism for inclusion behavior during electroslag remelting has been proposed.

Keywords: *Electroslag remelting (ESR); Non-metallic inclusions; Steelmaking; Thermodynamics of steel; Clean steel.*

1. Introduction

Electroslag remelting (ESR) is a special metallurgical process that is designed to reduce segregations and improve the steel's cleanliness. There are numerous reports on clean steel and inclusion formation [1–4], but studies concerning the ESR process conducted in the past decade have mainly focused on physical modelling, such as the melting rate, the melt droplet formation and heat transfer [5–16]. Among other things, the findings reveal that the slag layer has a heterogeneous temperature field and vortexes (turbulent flow) occur in the slag. However, research on the interactions between the steel, the slag and the non-metallic inclusions [17–21] is less common.

H11 is one of the most widely used hot-work tool steels. It is used in die casting, forging, plastic injection and extrusion. Because of the demanding conditions found in these applications, the quality of the tool material is essential for a long service life. The strict requirements, which include a fine microstructure with low segregations, low phosphorus and sulfur contents and a low inclusion content, can be achieved through ESR processing.

The ESR process is used for special materials that can afford the extra cost of processing, like special steels for energetics, hot-working tool steels, high-speed steels and nickel alloys. The products of the ESR process are high-purity, fine-grained ingots suitable for the most demanding applications. The concept of the process is as follows. The consumable electrode is dipped into the hot slag. The hot slag then melts the electrode. The formed metal droplets pass through the liquid hot slag into the metal pool below. The liquid pool is cooled by a water-cooled mold and then solidifies into the remelted ingot. During the droplets' journey through the liquid slag, thermochemical reactions with the ESR slag take place. The basic idea of the ESR furnace is that the consumable electrode, the slag and the remelted ingot form an electrical circuit [22]. The resistivity of the slag causes joule heating and is the main driving force behind the process. Joule heating through a molten slag layer maintains the slag temperature between 1700 °C and 2000 °C and melts one end of the electrode [23].

The aim of this work was to study the influence of the ESR process on non-metallic inclusions in the K0 size category, according to the DIN 50 602 standard for H11 tool steel.

2. Experimental

A study of the ESR process was performed. A 25-tonne consumable electrode of H11 was remelted into an ingot with a diameter of 1.0 m and a height of 4 m. The H11 steel was made using the EAF-VAD steelmaking process and was deoxidized by Al additions and treated with CaSi wire

**Corresponding author: jaka.burja@imt.si*

DOI:10.2298/JMMB160623053B

Table 1. *Chemical composition of H11 steel / wt%*

C	Si	Mn	Cr	Mo	V	Fe
0.33–0.43	0.80–1.20	0.20–0.50	4.75–5.50	1.10–1.50	0.30–0.60	Bal.

injections. In this study an industrial ESR with a protective nitrogen atmosphere was used. The chemical composition of the H11 tool steel is given in table 1.

The chemical composition of the slag used in the experiment is given in Table 2.

Table 2. *Chemical composition of the slag wt%*

CaF_2	CaO	Al_2O_3	SiO_2	MgO	FeO	TiO_2
40.1	33.1	22.2	2.8	1.5	0.1	0.2

Twelve samples were taken from the consumable electrode and twelve from the remelted ingot. There were four sets of samples: one from the bottom of the ingot, two from the middle and one from the top. This means that four of the samples were taken from the center, four from three quarters of the radius and four from the edge of the electrode and from the ingot, as seen in Figure 1.

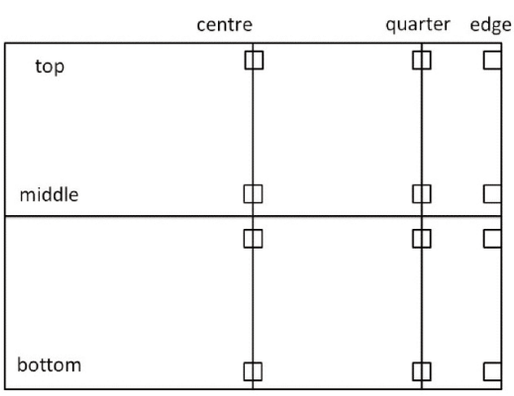

Figure 1. *Schematic representation of sampling areas*

The steel samples were grinded with sand papers and polished with 1-µm diamond paste to prepare for non-metallic inclusion observation. The samples were examined with a field-emission scanning electron microscope (FEG-SEM, JEOL JSM-6500F). Energy-dispersive X-ray spectroscopy (SEM EDS) was used to analyze the composition of the inclusions, and secondary-electron imaging (SEI) was used to measure the inclusion size. For each sample the analyzed surface was 3.7 mm^2, which makes a total analyzed surface, for the twelve samples, of approximately 44 mm^2. Inclusions with a diameter ≥ 5 µm were analyzed, while smaller inclusions were ignored, in accordance with the K0 category in the DIN 50 602 standard.

3. Results and discussion

The results of the non-metallic inclusion analysis are shown in Figure 2. It is clear that in our experiment the area that the non-metallic inclusions occupy is decreased after the ESR process.

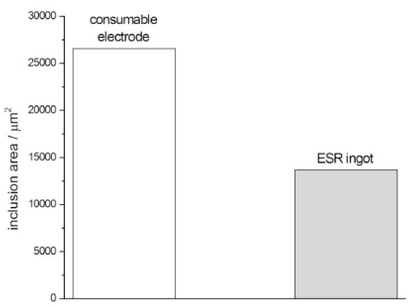

Figure 2. *Area of inclusions in the electrode and the ESR ingot*

Based on the results of the non-metallic inclusion analysis, the non-metallic inclusions were divided into five size categories and seven chemical composition categories:

1. Al_2O_3–MgO–CaO–(Mn,Ca)S+TiN partially modified spinel with attached sulfides and nitrides
2. Al_2O_3–MgO–CaO–(Mn,Ca)S partially modified spinel with attached sulfides (green)
3. (Mn,Ca)S+TiN sulfide with attached nitride
4. TiN nitride
5. (Mn,Ca)S–Al_2O_3–CaO–MgO sulfide with attached oxides
6. MnS manganese sulfide
7. Al_2O_3–SiO_2–MgO–CaO–(Mn,Ca)S silicate and other oxides with attached sulfides

The nitride inclusions observed in the electrode had either no other inclusions attached or had sulfides attached (Figure 3e, 3g). However, some of the nitride inclusions in the remelted ingot were also attached to oxides (fig 3. a).

Chang et al. [19] reported that there can be an oxygen increase in the ESR ingot due to the decomposition of oxides in the slag. The high temperatures that occur during the ESR process are up to 2000 °C [23] and are therefore thermodynamically suitable for oxide decomposition. Further analysis of the inclusions confirmed that there is a decrease in the number of inclusions after the ESR process. Furthermore, there is also a change in their chemical

composition. The silicon oxide that is present in all of the oxide inclusions in the electrode diminishes greatly after the ESR process. A possible explanation is that the rest of the sulfides, nitrides and oxides decompose in the steel melt during superheating. The non-metallic inclusion components like Al and O are dissolved in the melt. These dissolved elements form non-metallic inclusions and precipitate again during cooling and solidification (a process that is similar to the one described by Yang et al. [24-25]). In this way new inclusions can be formed in the remelted ingot, due to the decomposition of the old non-metallic inclusions.

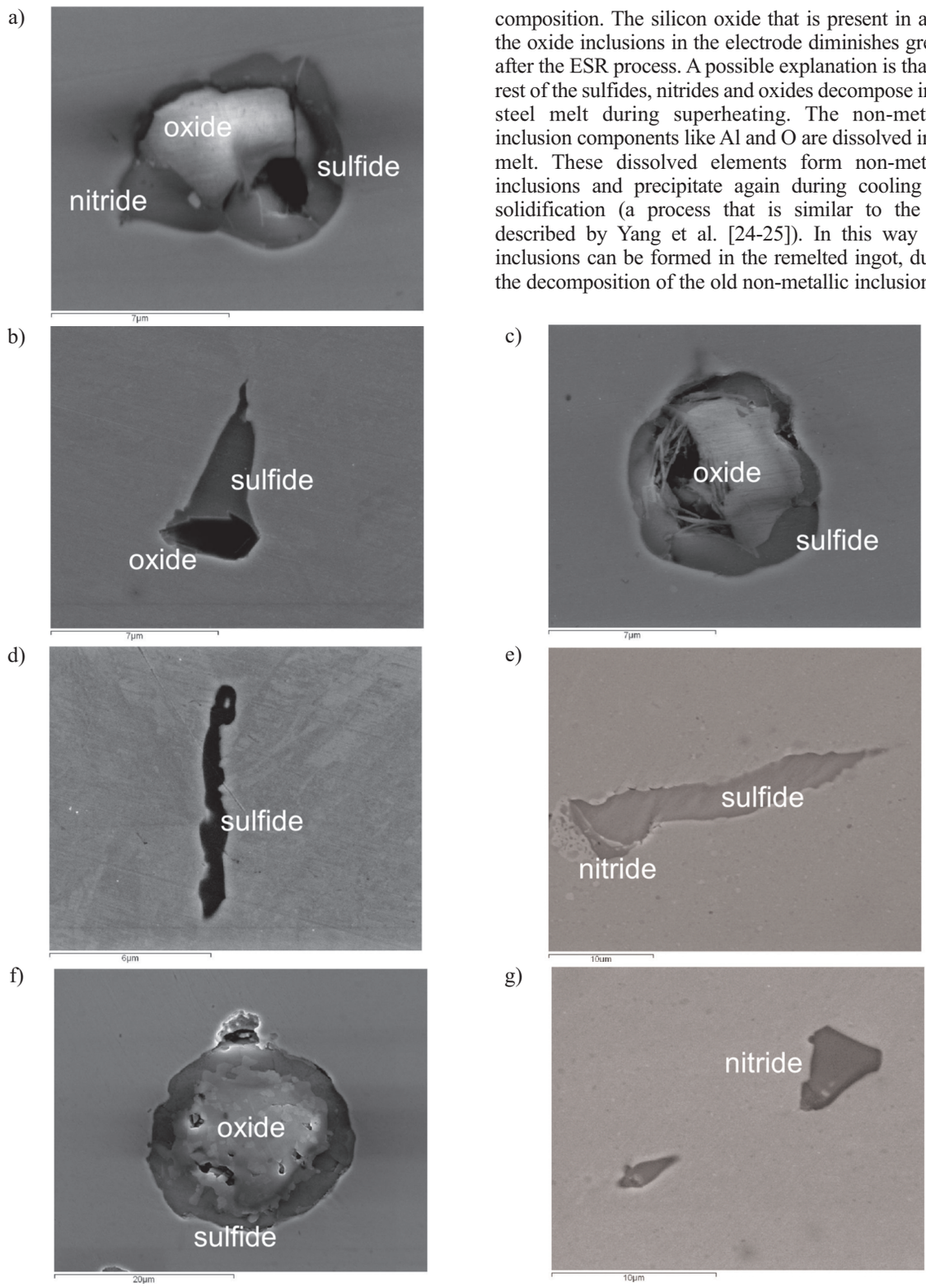

Figure 3. *Inclusions divided into seven chemical-composition-based categories: a) Al_2O_3–MgO–CaO–(Mn,Ca)S+TiN partially modified spinel with attached sulfides and nitrides (red); b) (Mn,Ca)S–Al_2O_3–CaO–MgO sulfide with attached oxides (purple); c) Al_2O_3–MgO–CaO–(Mn,Ca)S partially modified spinel with attached sulfides (green); d) MnS manganese sulfide (yellow); e) (Mn,Ca)S+TiN sulfide with attached nitride (blue); f) Al_2O_3–SiO_2–MgO–CaO–(Mn,Ca)S silicate and other oxides with attached sulfides; g) TiN nitride (cyan)*

The data for the thermodynamic calculations of the non-metallic-inclusion formation reactions were taken from the software HSC Chemistry 8.0 (pure substances) and were modified based on the Gibbs free energy changes resulting from the solution state in liquid iron in wt% (Sigworth et al. [25]). The interaction coeficients in dilute liquid iron solution are given in table 3 [26-27].

$Al_2O_3 = 2[Al] + 3[O]$ (1)

$\Delta G = \Delta H - T\Delta S = 1\,204.0\ kJ - T \cdot 388.0\ J/K$ (2)

$CaO = [Ca] + [O]$ (3)

$\Delta G = \Delta H - T\Delta S = 506.4\ kJ - T \cdot 66.5\ J/K$ (4)

$SiO_2 = [Si] + 2[O]$ (5)

$\Delta G = \Delta H - T\Delta S = 580.8\ kJ - T \cdot 98.5\ J/K$ (6)

$CaS = [Ca] + [S]$ (7)

$\Delta G = \Delta H - T\Delta S = 377.8\ kJ - T \cdot 30.5\ J/K$ (8)

The calculations show that higher temperatures favor oxide decomposition in the steel melt. For example, high temperatures and low oxygen potentials favor the formation of CaO. When the oxygen content is increased, the aluminum oxide becomes more stable, as shown in Figure 4.

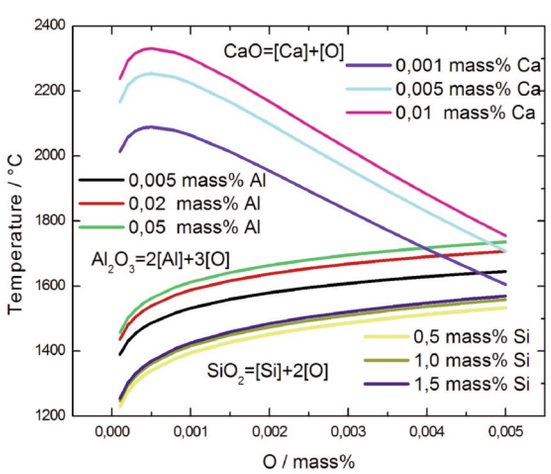

Figure 4. *Equilibrium lines for inclusion formation at different element contents with respect to the oxygen content and temperature*

The graph in Figure 4 also shows that the silicon oxide is the least stable at higher temperatures. Silicon oxide is not produced under these conditions and was not found in the non-metallic inclusions. The reaction of aluminum and calcium with oxygen results in the formation of Al_2O_3–CaO inclusions, which in turn lower the activity of both the Al_2O_3 and CaO, thus promoting further de-oxidation of the melt by aluminum and calcium. The curve for CaO formation is curved downwards at very low oxygen contents due to the high value of the interaction coefficients = -840 (table 3). Since calcium also forms stable sulfides, a part of the calcium is also used up by sulfur, depending on the oxygen content and the temperature, as shown in Figure 5.

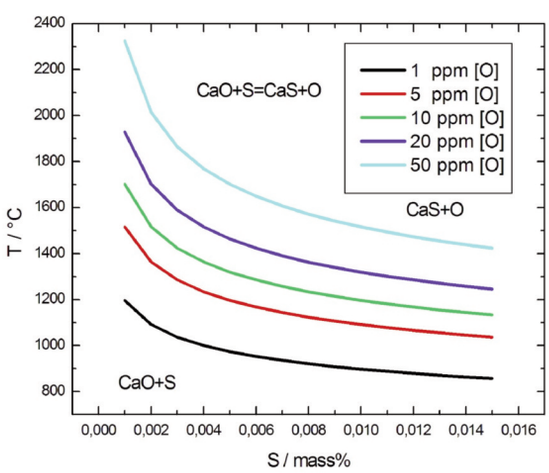

Figure 5. *Equilibrium lines for the formation of calcium oxide/sulfide with respect to the sulfur and oxygen contents at different temperatures*

The simultaneous formation of Al_2O_3, CaO and CaS results in complex oxysulfide non-metallic inclusions (as seen in Figure 3a, 3b), while the residual sulfur forms manganese sulfides. During solidification of the ESR ingot the precipitation of titanium nitrides also occurs and they are therefore often attached to the complex oxysulfide non-metallic inclusions.

Figure 6 displays the content of aluminum oxide, calcium oxide and calcium sulfide in non-metallic inclusions in the consumable electrode and the remelted ingot.

Figure 6 shows that the ESR process promotes desulfurization as the composition of the non-metallic inclusions shifts towards the CaO–Al_2O_3 system. This

Table 3. *Interaction coeficients in liquid iron solution at 1600 °C [26], 1550 °C* [27] and 1650 °C ** [27]*

	Si	Mn	Cr	Al	O	C	Ca	S
Al	0.0056*	0.035*	0.0096*	0.045	-6.6	0.091	-0.047	0.03
O	-0.131	-0.021	-0.04	-3.9	-0.2	-0.45		-0.133
Ca	-0.097	0**	0.014**	-0.072	-840**		-0.002	
Si	0.11	0,002	-0.0003	0.058	-0.23	0.18	-0.067	0.056
S	0.63	-0.026	-0.011	0.035	-0.27	0.11		-0.028
Mn	0	-0.0029	-0.091		-0.011	-0.07		

means that the constitution of the non-metallic inclusions found in the ESR ingot has been heavily influenced by the ESR slag. The non-metallic inclusions found in the electrode are the result of the entire steelmaking process and their origins can be traced to the oxidation of the silicon in the melt, deoxidation of the steel melt by aluminum, modification of the alumina inclusions by the CaSi wire, interactions between the melt and the refractory and precipitation during casting and solidification [1]. The non-metallic inclusions in the ESR ingot, on the other hand, formed in a much shorter time and are the result of reactions with the slag and decreased solubility of elements in the steel melt during cooling and precipitation during solidification. Figures 6 and 7 show that the amount of the third component, i.e., CaS or MgO, in the inclusions is reduced. The final result is the formation of non-metallic inclusions that are closer to the chemical composition of the slag.

If the chemical composition of the non-metallic inclusions is analyzed through the content of aluminum oxide, calcium oxide and magnesium oxide, as shown in the ternary diagram in Figure 7, the increase in Al_2O_3–CaO content in the non-metallic inclusions after the ESR process is obvious.

Dong et al. [17] studied the influence of ESR slags on the composition of non-metallic inclusions. They observed that there is an interaction between CaO in the slag, CaO in the inclusions and Ca in the liquid steel. The conclusion was that the original CaO in the inclusions will be gradually reduced by the Al dissolved in the liquid steel, and that the reaction time will be longer for a larger amount of CaO in the slag. However, in our case (as shown in Figure 7), the Ca and Al contents in the non-metallic inclusions increased, because the MgO content decreases. Dong et al. [17] also claimed that the content of SiO_2 in the non-metallic inclusions decreases due to the interaction of the slag and the metal, and that the inclusions are transformed into MgO–Al_2O_3 spinel-type inclusions. However, this is in contrast to our study shown in Figure 7, where the MgO content is lowered. The authors [17] also discussed the influence of the electrode-filling ratio on the non-metallic inclusion content, which increases with higher filling ratios. This is explained by the size of the metallic droplets in the slag and therefore decreased the slag-metal interaction surface. But it can also be argued, and Dong et al. [17] also concur, that a higher filling ratio requires a higher slag temperature in order to increase the electrode melting rate. As shown in Figure 4, higher temperatures cause more non-metallic inclusions to become unstable, and thus dissolving elements like Al and O back into the steel, and therefore avoid the transition from the metal to the slag.

The diagram in Figure 8 shows the number and type of non-metallic inclusions, depending on their size, plotted on the basis of an SEM analysis of the non-metallic inclusions.

The diagram clearly shows the change in the number of non-metallic inclusions as well as in their chemical composition. The decrease in the number of inclusions can be observed for all five size categories. Furthermore, the SiO_2-containing non-metallic inclusions that were predominant in the ESR electrode are no longer present in the ESR ingot, therefore suggesting the inclusion decomposition during melting

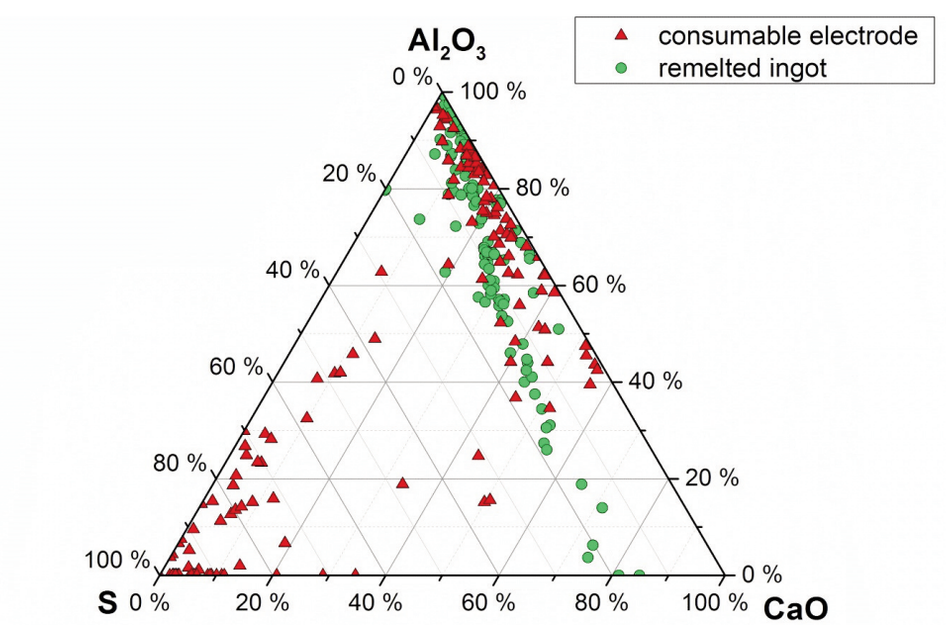

Figure 6. *Composition of non-metallic inclusions Al_2O_3–CaO–CaS*

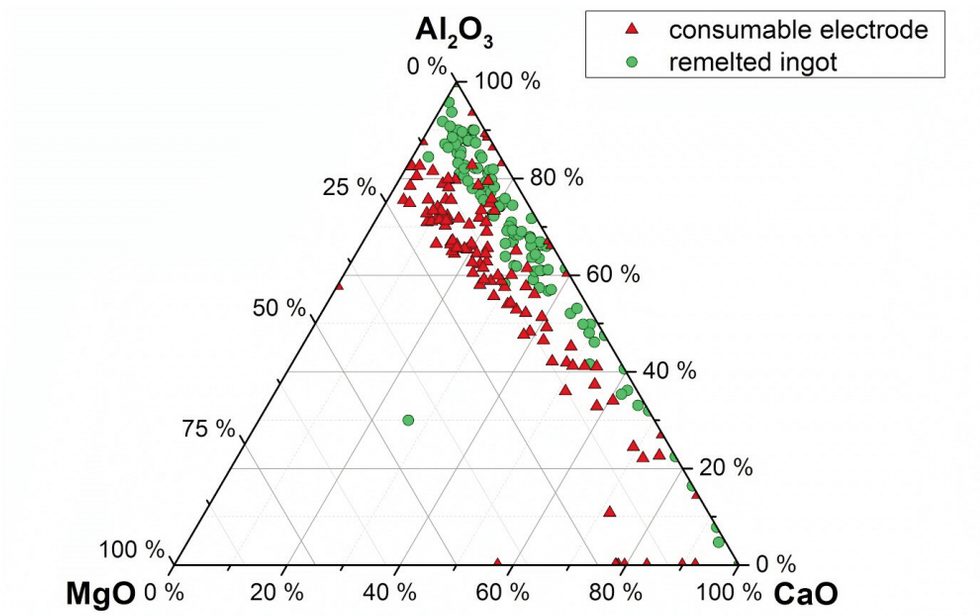

Figure 7. *Composition of non-metallic inclusions Al_2O_3–CaO–MgO*

and precipitation during the solidification mechanism.

A fraction of the non-metallic inclusions are absorbed by the ESR slag during the process, but more importantly a large part of the non-metallic inclusions decompose in the steel melt and precipitate during solidification. They are "regenerated" and are not carried through the slag layer. This is supported by calculating the Gibbs free energy for the formation of non-metallic inclusions in a dilute liquid iron solution. The curves in Figure 4 represent the temperatures above which the Gibbs free energy for the formation of oxides in equilibrium with a dilute iron melt is positive. This means that the non-metallic inclusions decompose at high temperatures and are possibly not removed by being dissolved in the slag.

The inclusion content depends on the inclusion formation/decomposition reaction that is greatly influenced by the slag temperature. It can be speculated that the higher the slag temperature by itself, not including more complex factors like a higher pool depth, the flow conditions, inclusion separation, higher solidification rate and more entrapped inclusions, can be attributed to a higher final inclusion content in the ingot. This speculation is based on the fact that the solubility of the elements is increased in the steel melt and that the oxides become thermodynamically unstable at high temperatures, therefore forming during cooling and solidification.

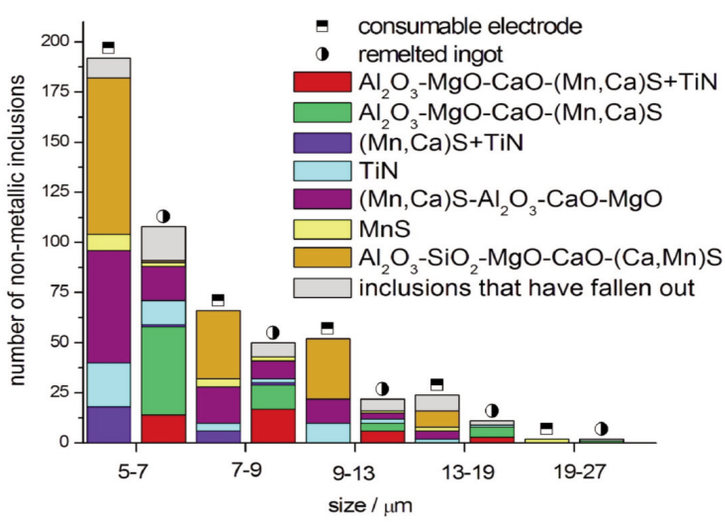

Figure 8. *Size distribution of non-metallic inclusions with type description*

4. Conclusions

In the studied experiment for the remelting of the H11 tool steel using slag based on CaF_2, CaO and Al_2O_3 with very low content of MgO and SiO_2 the ESR process had the following effects: The number of non-metallic inclusions in the steel as well as the area they represent on the sample surface decreased. The chemical composition of the non-metallic inclusions changed. The MnS content is strongly decreased, the SiO_2 is completely removed and the MgO is strongly reduced. The composition of the non-metallic inclusions shifts towards the Al_2O_3–CaO two-phase system with a small quantity of residual components. This is consistent with the slag composition. Due to the simultaneous formation of nitrides, oxides and sulfides the non-metallic inclusions in the ESR ingot also consist of oxysulfides with attached nitrides. The number of sulfide inclusions decreases.

References

[1] L. Zhang and B.G. Thomas: Metall. Mater. Trans. B, 37B (2006) 733–761.
[2] M. Faraji, D. P. Wilcox, R. Thackray, A. A. Howe, I. Todd,, P. Tsakiropoulos: Metall. Mater. Trans. B, 46B (2015) 2490–2502.
[3] D. Zhao, H. Li, C. Bao, J. Yang: ISIJ Int., 55 (2015) 2115–2124.
[4] L. Krajnc, P. Mrvar, J. Medved: Mater. Tehnol., 48 (2014) 923–929.
[5] Y. Dong, Z. Jiang, Y. Cao, D. Hou, L. Liang,: ISIJ Int., 55 (2015) 904–906.
[6] F. Liu, X. Zang, Z. Jiang, X. Geng, M. Yao: Int. J. Miner. Metall. Mater., 19 (2012) 303–311.
[7] W. Li, W. Wang, Y. Hu, Y. Chen: Metall. Mater. Trans. B, 43B (2011) 276–289.
[8] V. Weber, A. Jardy, B. Dussoubs, D. Ablitzer, S. Rybéron, V. Schmitt, S. Hans, H. Poisson: Metall. Mater. Trans. B, 40B (2009) 271–280.
[9] L. Z. Chang, X. F. Shi, J. Q. Cong, R. X. Wang: Ironmak. Steelmak., 41 (2014) 611–617.
[10] A. Kharicha, A. Ludwig, M. Wu: ISIJ Int., 54 (2014) 1621–1628.
[11] A. Kharicha, A. Ludwig, M. Wu: Mater. Sci. Eng. A, 413-414A (2005) 129–134.
[12] A. Mitchell: Mater. Sci. Eng. A, 413-414A (2005) 10–18.
[13] Y. Dong, Z. Jiang, H. Liu, R. Chen, Z. Song: ISIJ Int., 52 (2012) 2226–2234.
[14] Q. Wang, Z.u He, B. Li, F. Tsukihashi: Metall. Mater. Trans. B, 45B (2015) 2425–2441.
[15] Y.W. Dong, Z.H. Jiang, J.X. Fan, Y.L. Cao, D. Hou, H.B. Cao: Metall. Mater. Trans. B, 47B (2016) 1475–1488.
[16] Y.L. Cao, Y.W. Dong, Z.H. Jiang, H.B. Cao, D. Hou, Q.L. Feng: Int. J. Miner. Metall. Mater., 23 (2016) 399–407.
[17] Y.W. Dong, Z.H. Jiang, Y.L. Cao, A. Yu, D. Hou: Metall. Mater. Trans. B, 45B (2014), 1315–1324.
[18] A. Ahmed A. Fathy: Ironmak. Steelmak., 35 (2008) 458–464.
[19] L. Z. Chang, X. F. Shi, J. Q. Cong: Ironmak. Steelmak., 41 (2014) 182–186.
[20] E. Yu. Kolpishon, A. N. Mal'ginov, A. N. Romashkin, V. A. Durynin, S. Yu. Afanas'ev, E. V. Shitov, L. T. Afanas'eva, Yu. M. Batov: Russ. Metall., 2010 (2010) 489–93.
[21] E. A. Vorona, V. I. Chumanov: Russ. Metall., 2010 (2010) 505–509.
[22] B. Arh, B. Podgornik, J. Burja: Mater. Tehnol., 50 (2016) 971–979.
[23] U. B. Pal, C. J. MacDonald, E. Chiang, W. C. Chernicoff, K. C. Chou, J. Avyle, M. A. Molecke, D. Melgaard: Metall. Mater. Trans. B, 32B (2001) 1119–1128.
[24] L. Yang, G.G Cheng, S.J. Li, M. Zhao, G.P. Feng: ISIJ, 55 (2015) 1901–1905.
[25] L. Yang, G.G Cheng: Int. J. Miner. Metall. Mater., 24 (2017) 869–875.
[26] G. K. Sigworth, J. F. Elliott: Met. Sci., 8 (1974) 298–310.
[27] Y. H. Park, D. S. Kim, S. B. Lee: Metall. Mater. Trans. B, 36B (2005) 495–502.

UTICAJ PRETAPANJA U ELEKTRIČNIM PEĆIMA SA TEČNOM ŠLJAKOM NA NEMETALNE UKLJUČKE U H11 ALATNOM ČELIKU

J. Burja [a], F. Tehovnik [a], M. Godec [a], J. Medved [b], B. Podgornik [a], R. Barbič [c]

[a] Institute of Metals and Technology, Ljubljana, Slovenia,
[b] University of Ljubljana, Faculty of Natural Sciences and Engineering, Ljubljana, Slovenia
Rok Barbič, Metal d.o.o., Ravne na Koroškem, Slovenia

Apstrakt

U radu je proučavan uticaj pretapanja čelika u električnim pećima sa tečnom šljakom na sadržaj i sastav nemetalnih uključaka. Otkriveno je da je tokom pretapanja u električnoj peći dolazilo do smanjenja u sadržaju nemetalnih uključaka. Primećena je promena u hemijskom sastavu nemetalnih uključaka, dok je sadržaj aluminijuma i kalcijuma povećan. Kompleksnost uključaka je takođe rasla, pošto je bilo sve manje monofaznih uključaka posle procesa pretapanja. Na osnovu ovih rezultata i termodinamičke procene stvaranja nemetalnih uključaka, predložen je mehanizam ponašanje uključaka tokom pretapanja čelika u električnim pećima sa tečnom šljakom.

Ključne reči: *Pretapanja u električnim pećima sa tečnom šljakom (ESR); Nemetalne uključci; Proizvodnja čelika; Termodinamika čelika; Čist čelik*